RSC Advances

ROYAL SOCIETY OF CHEMISTRY

www.rsc.org/advances

Synthesis, characterization, and application of Fe_3O_4@SiO_2-NH_2 nanoparticles

Feng Liu [a b 1], Fuge Niu [a b], Ning Peng [a b], Yujie Su [a b *], Yanjun Yang [a b *]

[a] State Key Laboratory of Food Science and Technology, Jiangnan University, Wuxi 214122, PR China

[b] School of Food Science and Technology, Jiangnan University, Wuxi 214122, PR China

Abstract

Magnetic Fe_3O_4@SiO_2-NH_2 nanoparticles were synthesized, characterized and applied as magnetic adsorbing carrier to separate ovotransferrin (OVT) from chicken egg white in this paper. Properties of the particles were characterized, results showed that silica shell and terminal amino groups were successfully decorated to the Fe_3O_4 core; the mean diameter of the modified particles was about 210 nm and the isoelectric point (pI) was approximately 9.25; in addition the particles displayed desirable magnetic properties, excellent dispersibility and high stability. The particles performed satisfactorily in the separation of OVT and the maximum adsorption loading reached 77.2 mg/g in 30 min at 40°C. Moreover Fe_3O_4@SiO_2-NH_2 nanoparticles were very stable after repeated adsorption-desorption experiments. OVT separated by Fe_3O_4@SiO_2-NH_2 nanoparticles displayed strong ability of binding iron and had a high purity. Besides, the recovery of OVT separated from egg white was calculated to be 84.62%. In addition, the nanoparticles showed desirable repeatability in repeated adsorption-desorption experiments. Hence Fe_3O_4@SiO_2-NH_2 nanoparticles were promising to scale up the separation of OVT from chicken egg white due to the huge advantages of high dispersion, high reactivity, and easy separation.

Keywords: magnetic nanoparticles; isoelectric point; separation; ovotransferrin

1. Introduction

In recent decades, functionalized magnetic nanoparticles had gained much attention due to their magnetic properties, high surface area, low cost, non-toxicity and biocompatibility. Usually the magnetic core which provided a more convenient and effective separation or deliver medium was coated with a layer of functional

silica since the silica shell not only could help to stabilize the nanoparticles in a specific condition but also was readily modified with other functional groups for further application as the surface of silica-coated magnetic nanoparticles was hydrophilic [1]. Silica coating made it easy to control the size and morphology of particles according to Stober method [2], the thickness of silica shell could also be easily controlled by adjusting the concentration ratio of ammonium to tetraethyl orthosilicate [1,3]. Moreover, these coated magnetic nanoparticles were redispersible in water without the need of adding other surfactants owing to the negative charges on the silica shell. In spite of the advantages of silica-coated magnetic nanoparticles, the course of synthesis reaction might be time-consuming as reported [4], even more than 30 hours were needed to synthesis amino-functionalized single magnetic core-silica shell composites [5]. In order to save reaction time method according to Zhang [4] was improved and only about 15 h were cost during the whole reaction in this study.

Iron oxide-based amino-functionalized magnetic nanoparticles demonstrated outstanding charge matching capability and special magnetic properties, which had made them suitable for a wide range of applications in drug targeting, protein purification and water treatment [3]. On account of the functionality and superparamagnetism of magnetic nanoparticles, they could combine with the aimed protein selectively to the active groups on the surface of the particles, then the particles-proteins could be separated rapidly with an external magnet. Kinds of functional magnetic nanoparticles had been used in the separation of protein according to some reports, for example polysaccharide-modified iron oxide nanoparticles were used to adsorb BSA and achieved a high desorption percentage [6]; Functional Fe_3O_4 nanoparticles conjugated with carboxymethyl chitosan were used as adsorbing carrier for the purification of lysozyme and showed excellent binding of a large amount of lysozyme [7]. However, to the author's knowledge, their studies might be more reasonable if they had considered the stability of the functional

nanoparticles after repeated adsorption-desorption experiments for certain times. A lot of cost would be saved if the modified nanoparticles could be recycled for enough times. In this study Fe_3O_4@SiO_2-NH_2 nanoparticles were applied in separation of ovotransferrin (OVT) from egg white and it was hoped that the problem above would be solved.

OVT, a member of transferrins with a isoelectric point (pI) of 6.0, accounts for about 13% of total protein in chicken egg white and possesses a capability to reversibly bind two Fe^{3+} ions concomitantly with one bicarbonate anion [8,9]. Due to its ability to bind and sequester iron (Fe^{3+}) which is essential for the growth of many microorganisms such as *Escherichia coli*, OVT owes strong antimicrobial activity similar to serum transferrin [10,11]. Therefore OVT could be used as food additive in function food, dairy productions or other meat product owe to its excellent antimicrobial activity and promotion in iron adsorption.

Up to date many procedures to separate OVT had been developed, mainly on a laboratory scale. Traditional ways such as ammonium sulfate precipitation or ultrafiltration were used in the preparation of OVT from chicken egg white, but the purity of protein isolated was particularly low and the protein was even partly degenerated [12]. Afterwards, chromatography was explored to solve the existing problems. Although the protein was prevented from being degenerated and the purity got improved by chromatography, these methods were all laboratory studies and could not be scaled up, additionally the recovery of OVT was low [13]. To solve the problems above, functionalized Fe_3O_4@SiO_2-NH_2 magnetic nanoparticles with magnetically responsive core and functionalized groups were firstly introduced in the separation of OVT from egg white.

To prepare appropriate functional magnetic nanoparticles for separation of OVT from chicken egg white, modified chemical co-precipitation method was used for preparing magnetic Fe_3O_4 core, then silica shell was coated on the magnetic core in alkaline solution according to the Stober method [2,14], finally the particles were

modified with 3-Aminopropyl trimethoxysilane (APTMS) to introduce amine groups by sol-gel co-condensation method. The size, pI, functional groups, magnetic properties and morphology of the particles were studied. Then Fe_3O_4@SiO_2-NH_2 nanoparticles were used for purifying OVT from egg white and effects of medium pH and temperature on the maximum protein adsorbing onto the surface of nanoparticles were studied. In addition, the purity of the eluted protein was assessed by sodium dodecyl sulfate polyacrylamide gel electrophoresis (SDS-PAGE) and the ability of combining Fe^{3+} ion was evaluated by ultraviolet adsorption of protein and ferric chloride mixed solution. Finally the repeatability of Fe_3O_4@SiO_2-NH_2 nanoparticles in the repeated adsorption-desorption experiments was studied.

2. Experiment

2.1. Materials

Iron (III) chloride hexahydrate ($FeCl_3 \cdot 6H_2O$), iron (II) sulfate heptahydrate ($FeSO_4 \cdot 7H_2O$), 25% ammonia solution ($NH_3 \cdot H_2O$), ethanol (C_2H_5OH), tetraethyl orthosilicate (TEOS), APTMS were of analytical reagent grade and used without further purification. Fresh chicken eggs were purchased from local supermarket. Highly pure water with an electrical resistivity of 18.2 $M\Omega \cdot cm^{-1}$ was used through all the experiment.

2.2. Synthesis of Fe_3O_4@SiO_2-NH_2 nanoparticles

Firstly, 0.8 g $FeSO_4 \cdot 7H_2O$ and 0.9 g $FeCl_3 \cdot 6H_2O$ were dissolved in mixed solution of water (200 mL) and ethanol (40 mL) under the condition of vigorously stirring. After reacting for 30 minutes $NH_3 \cdot H_2O$ (15 mL) was added to the solution slowly as precipitating agent. Another 15 min was needed for the reaction once the color of the mixed solution turned black. The obtained Fe_3O_4 magnetic nanoparticles were washed several times with water and then dried in vacuum for further use.

Secondly, 80 mg magnetic nanoparticles were dispersed in mixed solution of water (10 mL) and ethanol (150 mL) by ultrasonic for 30minutes. Then $NH_3 \cdot H_2O$ (3 mL) and TEOS (2 mL) were added into the system and the pre-hydrolysis of TEOS

would last for 4 h under vigorously stirring at 30°C.

Finally, the reaction performed another 4h prior to the addition of APTMS. Afterward the precipitate was collected, washed several times, dried in vacuum and reserved for next step. The whole reaction (as scheme 1 showed) was performed under nitrogen atmosphere.

2.3. Characterization of Fe_3O_4@SiO_2-NH_2 nanoparticles

Fourier Transform Infrared (FTIR, Nicolet iS10, Thermo Scientific Corporation) was used to determine the chemical functionalities on the surface of Fe_3O_4@SiO_2-NH_2 nanoparticles. The samples were mixed with potassium bromide (KBr) powder and then the mixtures were made into pellet under high pressure. The sample pellet were scanned from 4000 to 400 cm^{-1}. Pure KBr acted as blank. The sizes of modified nanoparticles in different pH environments were measured in order to assess the stability. Each measurement was performed for three times. Besides the zeta potential of the nanoparticles vs. pH adjusted by HCl (0.5 M) and NaOH (0.5 M) was measured by Zeta-sizer Nano Series (Nano-ZS, Malvern Instruments Ltd., UK) to evaluate the pI of the nanoparticles. 10 runs with 15 cycles per run were applied. The pH value at which the Zeta potential was 0 mV was the pI. In addition, the effect of APTMS dosage on pI of the particles was studied. Particles size, morphology and structure of Fe_3O_4@SiO_2-NH_2 were evaluated using JEOL JEM-2010 (HT) TEM operated at 200 kV, (TEM). For the TEM investigations, the samples were dissolved in ethanol and deposited by placing two drops of nanoparticle suspension onto a carbon-covered copper-grids, followed by drying at room temperature. The X-ray diffraction (XRD) patterns of magnetite nanoparticles were collected by XRD measurements using CuKα radiation (=1.5406˚A) at 40 kV/40 mA on a Shimadzu 1001/SC diffractometer, in the Bragg-Bretano geometry in the 2θ range of 20-80˚ (scan speed 4 deg./min, preset time 0.6 s and step 0.02 deg.). The concentration of iron oxide in the functionalized MNPs was investigated by thermo-gravimetric analysis (Q50, TA Instruments, USA) under Nitrogen atmosphere at a heating rate of

141 25 °C/min.

142 *2.4. OVT purification from egg white*

143 Chicken egg white was diluted with 2 volumes of distilled water after separated
144 from fresh eggs, then the mixture was adjusted to pH 4.5 with HCl (0.05 M).
145 Afterward the solution was kept 4°C for 1h to precipitate ovomucin. Finally the
146 solution was centrifuged at 4°C at 8000 rpm for 30 min. The albumen buffer solution
147 was gotten by mix the supernatant fluid and 2 volumes phosphate buffer.

148 10 mg of Fe_3O_4@SiO_2-NH_2 nanoparticles and 10 mL of albumen buffer solution
149 (pH 6.8, 7.0, 7.2, 7.4, 7.6, 7.8, 8.0) were mixed in a conical flask (50 mL), afterward
150 the mixture was shaken in a thermostated shaker (30°C, 180 rpm) for certain time,
151 respectively. The particles-proteins were separated under magnetic field and washed
152 several times with distilled water. Finally the protein was eluted from the
153 nanoparticles with phosphate buffer (pH 5.0). At the end of desorption separated the
154 particles and collected the supernatant. The manipulation demonstration was
155 displayed in scheme 2. The concentration of supernatant solution was calculated
156 according to the absorbency at 465 nm by ultraviolet spectrophotometer. Each
157 measurement was performed for three times for reliable data. Effects of the medium
158 pH and temperature on the adsorbing process were studied.

159 The amount of OVT that was adsorbed onto the particles was calculated as

160 $$Q = \frac{V(C1 - C2)}{m} \quad (1)$$

161 Where Q was the amount of OVT adsorbed on the particles (mg/g), V was the volume
162 of OVT buffer solution (mL), C_1 and C_2 were the concentrations of OVT in the initial
163 egg white solution and in the supernatant after adsorption (mg/mL), respectively, m
164 was the mass of Fe_3O_4@SiO_2-NH_2 nanoparticles used in this adsorption experiment
165 (g). All data used in this equation were averages of duplicated experiments.

166 *2.5. Studies on the eluted protein*

167 SDS-PAGE with 10% separating gel and 5% stacking gel was conducted to
168 examine the purity of the eluted protein solution. SDS-protein samples were heated at

95°C for 4 min. Afterward the samples were subjected to electrophoresis at 80 V (until the bromophenol blue bland pass the stacking gel) and 120 V (until the bromophenol blue bland pass the separating gel) per gel. After electrophoresis, the gel was stained with 0.2 g/L Coomassie Brilliant Blue R-250 for 1h and destained with 50 mL/L ethanol and 100 mL/L acetic acid. Molecular weight markers (Sigma Chemical Co.) were used to estimate the molecular weight of proteins.

The recovery of separated OVT from egg white was calculated following the equation below:

$$R = \frac{V_1 \cdot c_1}{V_0 \cdot \rho \cdot c_0} \quad (2)$$

Where R was the recovery of OVT from egg white (%), V_0 and V_1 were the volume of egg white and eluted protein solution (mL), respectively, ρ was the density of egg white (g/mL), C_0 was the content of OVT in egg white (%), C_1 was the concentration of eluted protein solution (g/mL). All data used in this equation were averages of duplicated experiments.

The iron-binding ability of OVT was studied according to Graham and Bates [13]. Firstly, certain OVT was dissolved in 0.02M Tris-HCl buffer containing little $NaHCO_3$ and NaCl which contributed to the binding between OVT and iron. Then the OVT solution and $FeCl_3$ solution were mixed with different ratio of iron and OVT at room temperature. After reacting for 10 mins, differences of the solutions in absorbency at 465 nm were measured by ultraviolet spectrophotometer.

2.6. Repeatability of Fe_3O_4@SiO_2-NH_2 nanoparticles in the repeated adsorption-desorption experiments

The adsorption and desorption cycles were repeated thirty times using the same batch of Fe_3O_4@SiO_2-NH_2 nanoparticles to determine the reusability of the materials. After adsorption and desorption the Fe_3O_4@SiO_2-NH_2 nanoparticles were separated, collected and washed with deionized water for three times. Repeated the adsorption and desorption experiment and calculated the maximum adsorption of OVT onto the surface of Fe_3O_4@SiO_2-NH_2 nanoparticles every five times and weight loss of

197 Fe_3O_4@SiO_2-NH_2 nanoparticles before and after separation.

198 **3. Results and discussion**

199 *3.1. Properties of Fe_3O_4@SiO_2-NH_2 nanoparticles*

200 The silica shell on the surface of Fe_3O_4@SiO_2-NH_2 nanoparticles not only
201 protected the magnetic cores against aggregating, but also made it easy to introduce
202 new functional groups [15]. In this study, properties of both Fe_3O_4@SiO_2-NH_2
203 nanoparticles and naked magnetic Fe_3O_4 nanoparticles were studied.

204 FTIR spectra of Fe_3O_4@SiO_2-NH_2 nanoparticles and naked magnetic Fe_3O_4
205 nanoparticles were performed to confirm the existing of silica shell and terminal
206 amino (Fig. 1). The characteristic peak corresponding to the stretching vibration of
207 Fe-O bond was shifted to lower wavenumbers of 585 cm^{-1} after decorating compared
208 to that of 595 cm^{-1}, suggesting that Fe_3O_4 was influenced by Si-O of the silica shell.
209 As Yang [16] reported, the peak corresponding to the stretching vibration of Fe-O
210 bond was shifted to 701 cm^{-1} from 570 cm^{-1} after decorated graphene oxide due to the
211 effect of -COO^- on the graphene oxide surface. In comparison with the curve of pure
212 Fe_3O_4, the sharp peak at 1090 cm^{-1} was assigned to the Si-O-Si asymmetric stretching
213 vibration which indicated the formation of silica shell on the surface of Fe_3O_4. The
214 broad characteristic band around 3400 cm^{-1}, which corresponded to -NH stretching
215 modes, was also related to the bonded APTMS molecule. In addition, the typical peak
216 at 1610 cm^{-1} was also attributed to amino groups, indicating that there was terminal
217 -NH_2 on the surface of particles after decorating. The peak at 835 cm^{-1} could be
218 assigned to the bending vibration of C-H from APTMS. That was to say, APTMS was
219 successfully introduced onto the surface of Fe_3O_4@SiO_2 particles.

220 Stability was a crucial requirement for almost any application of magnetic
221 nanoparticles. Diameter was generally used as an index to assess the stability of
222 nanoparticles. The average diameter of Fe_3O_4@SiO_2-NH_2 nanoparticles was about
223 220.1nm at the pH of 7.0 as the results revealed (Fig. 2). The medium pH did not
224 exert an effect on the diameter apparently according to the results. The reason was

thought to be the silica shell, which effectively prevented the agglomerating between Fe_3O_4 cores. Such small magnetic nanoparticles tended to form agglomerates to reduce the energy associated with the high surface area to volume ratio of the nanoparticles. Moreover, naked metallic nanoparticles were chemically highly active and easily oxidized in air, resulting generally in loss of magnetism and dispersibility [17]. Thus a silica layer, which is impenetrable so that oxygen can not reach the surface of the magnetic particles, is necessary to improve the stability of the naked magnetic nanoparticles against oxidation and acid erosion during or after the synthesis. Besides, it is noteworthy that in many cases the silica protecting shell not only stabilize the nanoparticles, but can also be used for further functionalization. In addition, no matter in acid or alkaline solution the modified nanoparticles displayed narrow size distributions as the average particle dispersion index (PDI) was 0.3334, displayed in Tab. 1. The distribution of particles sizes was also one of the parameters influencing the magnetic properties. Since the distribution of the blocking temperatures depended on the particle sizes, a narrow particle size distribution will resulted in a narrow range of blocking temperatures and therefore ideal magnetic behavior for many applications.

Electrokinetic properties and zeta potential of modified nanoparticles exerted an important effect on the application of magnetic nanoparticles. The zeta potential not only characterized the stability of the electrostatically stabilised dispersion, namely a high zeta potential (positive or negative) implies stable systems [15], but also revealed the pI (the pH value at which the zeta potential equal zero) of the functional nanoparticles. The pI of unmodified Fe_3O_4 magnetic nanoparticles was about 5.0 while Fe_3O_4@SiO_2-NH_2 nanoparticles was about 9.25 according to Fig. 3. The pI was significantly depended on the functional groups on its surface. At high density of H^+ ions the formation of NH^{3+} groups was induced on the surface of Fe_3O_4@SiO_2-NH_2 nanoparticles, which led to the positive charge on the surface of the modified particles. While in alkaline solution, situation was contrast. Due to the strong ability of

combining H^+, Fe_3O_4@SiO_2-NH_2 nanoparticles had a higher pI than Fe_3O_4 magnetic nanoparticles.

Effect of APTMS dosage on the zeta potential of Fe_3O_4@SiO_2-NH_2 nanoparticles was not negligible as displayed in Fig. 4. It could be concluded from the curves that once increasing the addition of APTMS would lead to the shifting of electrokinetic curve towards higher pH. With the increase of APTMS amount in the range of 0-0.05 mL the pI of Fe_3O_4@SiO_2-NH_2 particles was gradually increased. It was attributed to the condensation polymerization of APTMS onto the surface of nanoparticles, and due to the increase of APTMS dosage more terminal amino groups generated. Hence the pI tended to be higher along with the increase in the amount of APTMS. When the dosage of APTMS reached 0.05 mL increasing the addition of APTMS did not exert an influence on the pI of nanoparticles greatly. This might be contributed to the self-condensation reaction of APTMS instead of condensation polymerization onto the surface of particles when the concentration of APTMS got higher. Therefore the amount of amino groups on the surface of particles would not increase substantially when increased the dosage of APTMS.

The morphologies and diameters of the nanoparticles of Fe_3O_4 and Fe_3O_4@SiO_2-NH_2 nanoparticles were learned by TEM analysis as shown in Fig. 5. It could be observed that both naked Fe_3O_4 and Fe_3O_4@SiO_2-NH_2 nanoparticles were nearly spherical and got smooth surface. The mean diameter of Fe_3O_4@SiO_2-NH_2 nanoparticles was 261.3 nm and the result was not fully consistent with the result according to DLS. The main reason might be that the solvent did exert a significant impact on the sizes of the samples since the samples were dispersed in ethanol during TEM analysis while in water during DLS analysis. Besides it was noticeable that the mean diameters of the nanoparticles increased from 18.3 nm to 261.3 nm after decorated by TEOS and APTMS. It was caused by the silica shell and amino groups on the surface of the Fe_3O_4 core. It could be clearly observed that there was a thin layer of 40.2 nm enwrapped on the surface of Fe_3O_4 magnetic core. Moreover, the

magnetic core was thought to be composed of several naked Fe_3O_4 nanoparticles. As a result, the mean diameter of Fe_3O_4@SiO_2-NH_2 nanoparticles was far larger than those of naked Fe_3O_4 nanoparticles. In addition, the Fe_3O_4@SiO_2-NH_2 nanoparticles displayed satisfactory uniformity and dispersibility.

The XRD measurements were performed with the dried powder samples of naked Fe_3O_4 and Fe_3O_4@SiO_2-NH_2 nanoparticles to identify the crystal phases. As showed in Fig. 6, all the peak positions at 30.1 (200), 35.4 (311), 43.0 (400), 53.7 (422), 57.2 (511), and 62.4 (440) were consistent with the standard X-ray data for Fe_3O_4 magnetite phase (JCPDS no. 19-0629) [18]. There was a decrease of peak intensity after modifying, which was attributed to the silica shell enwrapped on the surface of the particles. In addition, no additional peaks for other phases were detected, indicating that no redundant reaction had occurred between the core and shell.

TGA analyses were usually used to determine the content of functional groups and magnetic content of the particles. According to Fig. 7, the TGA curve of naked Fe_3O_4 nanoparticles showed a weight loss of 5.05% from 25^{o}C to 900^{o}C.While the Fe_3O_4@SiO_2-NH_2 nanoparticles showed a weight loss of 12.76%. The reason was possibly that compared with naked Fe_3O_4 nanoparticles there were release of hydroxyl ions and decomposition of aminopropyl groups on the Fe_3O_4@SiO_2-NH_2 nanoparticles except water thermo-desorption. It was also confirmed that the Fe_3O_4 nanoparticles was successfully decorated by TEOS and APTMS. In addition, it could be easily concluded that the magnetic content of Fe_3O_4@SiO_2-NH_2 nanoparticles was 8.12% less than that of naked Fe_3O_4 nanoparticles. Although the silica shell and functional groups might reduce the magnetic content and magnetic properties of the naked Fe_3O_4 nanoparticles slightly, the Fe_3O_4@SiO_2-NH_2 still showed good magnetization, which suggested their suitability for magnetic targeting and separation. As the inset in Fig. 7 showed that the Fe_3O_4@SiO_2-NH_2 nanoparticles could be attracted quickly by an external magnet and it confirmed the desirable magnetic

properties of the nanoparticles. Besides it was noticeable that the nanoparticles showed excellent dispersibility as the nanoparticles dispersed again in aqueous solution rapidly once the external magnetic field was removed. Therefore the Fe_3O_4@SiO_2-NH_2 nanoparticles presented excellent magnetic properties and had desirable potential application as recyclable nanomaterials.

3.2. Separation of OVT from egg white

The adsorption isotherms of OVT on the Fe_3O_4@SiO_2-NH_2 nanoparticles were showed in Fig. 8. The adsorption equilibrium of OVT on the Fe_3O_4@SiO_2-NH_2 nanoparticles fitted well with Langmuir model, at the beginning of adsorption, the adsorption amount of protein increased rapidly within 20 min and then reached the maximum value at about 40 min. The rate of adsorption significantly increased with the raise of temperature at the beginning of adsorption. The reason was that once elevating the temperature the Brownian movement would get violent and the risk of collision between protein and particles also got increasing as a result. Moreover, the maximum adsorption capacity of the particles for OVT increased from 54.5 mg/g to 77.2 mg/g with increasing temperature from 20^{o}C to 40^{o}C. This could be attributed to the strengthening of chemical interaction between the particles and the OVT molecules once the temperature increased. So a higher temperature was favorable to adsorption, but raising the temperature did have its defect, the OVT in egg white could not bear high temperature and might get degenerated.

As the adsorption of OVT onto the surface of particles was highly sensitive to environmental solution's pH, effect of the medium pH on the maximum adsorption of OVT onto nanoparticles was studied (Fig. 9). The maximum adsorption reached 77.2 mg/g at pH 7.4, and the adsorption would decrease when the pH was greater or less than 7.4. It was known that OVT had a pI of 6.1 [19], therefore the pH value of the aqueous solution had a great influence on the surface electric potential of OVT. The protein was negatively charged at pH > 6.0 and positively charged at pH < 6.0. Meanwhile the pI of Fe_3O_4@SiO_2-NH_2 nanoparticles was measured to be 9.25 and

hence the particles were negatively charged at pH > 9.25 and positively charged at pH < 9.25. Nanoparticles with positive charge would adsorb protein with negative charge by electrostatic interaction when the pH value was between the isoelectric points of protein and nanoparticles. The more charge the protein and particles carried, the stronger the electrostatic interaction was, consequently the larger the maximum adsorption was.

The recovery of OVT separated from egg white was calculated according to formula (2). The ρ of egg white is 1.10 g/mL on the basis of the experiment. As Gustavo Martos [20] revealed egg protein content was approximately 10% in egg white and OVT accounted for 13% in the whole egg white proteins [21]. According to the measurement, c_1 was calculated to be 12.1×10^{-3} g/mL based on standard curve, V_0 and V_1 were 1mL and 10 mL. Therefore Q=84.62%. That was to say, 84.62% of OVT in egg white was extracted in this experiment. In comparison with the recovery of 78% reported by C. Gue´rin-Dubiard [22], we could conclude that it was difficult to get high recovery of OVT from egg white by ion-exchange chromatography due to the gap between medium pH and OVT pI.

3.3. Quality of eluted protein

The purity of eluted OVT was determined by SDS-PAGE electrophoresis. Four major proteins: OVT, lysozyme, ovalbumin and ovoinhibitor were detected in the egg white solution according to Fig. 10. The eluted OVT had high purity after adsorption and desorption by Fe_3O_4@SiO_2-NH_2 nanoparticles since only one band, a molecular weight of about 78 KDa, was detected by SDS-PAGE. According to the results, it was also verified that pH of the adsorption solution did exert a great effect on the maximum adsorption of proteins onto the surface of nanoparticles. It was noteworthy that the electrophoretic band was darker and wider than the other when the pH of chicken egg white equal to 7.4, which means the best pH of adsorption of OVT from chicken egg white was 7.4. Most of the eluted OVT was proved to be apo-OVT as revealed by Fig. 11. Adding $FeCl_3$ to OVT solution led to the formation of holo-OVT

365 which was a pink iron-OVT complex [23] and had maximum adsorption peaks at 465
366 nm. There was a linear relationship between absorbency and the molar ratio of
367 iron/OVT until the molar ratio reached the maximum iron-binding rate. It could be
368 concluded that the maximum iron-binding rate was 1.7 instead of a theoretical
369 maximal binding rate of 2 [24]. The reason might be that original OVT in egg white
370 was not total iron-unsaturated. That was to say, separated OVT which owned a high
371 capacity to combine with iron maintained mostly original functional performance.

372 *3.4. Repeatability of Fe_3O_4@SiO_2-NH_2 nanoparticles*

373 Repeatability was a crucial index of the magnetic adsorbent used in affinity
374 separation. To evaluate the repeatability of Fe_3O_4@SiO_2-NH_2 nanoparticles,
375 repeated adsorption-desorption experiments were performed for thirty times using
376 the same batch of Fe_3O_4@SiO_2-NH_2 nanoparticles for OVT separation. The
377 maximum adsorption of OVT onto the surface of Fe_3O_4@SiO_2-NH_2 nanoparticles
378 was measured every five times. According to Fig. 12, after thirty times of uses, there
379 was only a bit of loss in the adsorption capacity of Fe_3O_4@SiO_2-NH_2 nanoparticles
380 and the maximum adsorption of OVT still remained more than 70 mg/g, which
381 indicated that the nanoparticles were very stable after repeated uses and owned well
382 repeatability. Thus Fe_3O_4@SiO_2-NH_2 nanoparticles could be used as affinity
383 materials in the separation of OVT due to their high adsorption capacity and
384 satisfactory repeatability.

385 The recovery of nanoparticles in the repeated adsorption-desorption experiments
386 was also one of the most important index of the repeatability. Here the recovery of
387 nanoparticles was investigated by measuring the weight of the nanoparticles after
388 every five cycles. According to Fig. 13, there was always a weight loss of the
389 nanoparticles after every adsorption-desorption cycles. The reason was likely to be
390 that the decrease of magnetic content and mangnetic responsiveness of
391 Fe_3O_4@SiO_2-NH_2 nanoparticles once it completed the binding of OVT would lead to
392 the loss slightly during the washing and recycling of nanoparticles. The recovery of

Fe_3O_4@SiO_2-NH_2 nanoparticles decreased from 10 mg to 7.03 mg after thirty-times repeated adsorption- desorption experiments. It could be concluded that it was the benign magnetic properties of modified nanoparticles that contributed to the satisfactory recovery. Hence the combination of benign magnetic properties, the high adsorption capacity of binding OVT on the surface of the nanoparticles, and good repeatability of the nanoparticles in repeated adsorption-desorption experiments suggested that the Fe_3O_4@SiO_2-NH_2 nanoparticles were ideal candidates of magnetically targeted protein carrier.

4. Conclusions

Well-dispersed Fe_3O_4@SiO_2-NH_2 magnetic nanoparticles with benign stability, satisfactory magnetic responsiveness and high adsorption capacity for OVT were synthesized by a mild and time-saving method. The decorated nanoparticles with uniform core-shell structure showed excellent stability and dispersibility both in acid and alkaline solution. Satisfactory magnetic responsiveness made it easy and rapid to separate OVT by the nanoparticles. It turned out that the Fe_3O_4@SiO_2-NH_2 nanoparticles were qualified to separate OVT from egg white and displayed a high adsorption loading. The OVT separated by the nanoparticles showed satisfactory purity and good activity. In addition, the nanoparticles showed desirable repeatability in repeated adsorption-desorption experiments. Hence Fe_3O_4@SiO_2-NH_2 nanoparticles were ideal candidates of magnetically targeted protein carrier for separating OVT from chicken egg white due to the huge advantages of easy separation, good separating effect, and satisfactory repeatability.

Acknowledgements

This experimental study was financially supported by the Chinese National High Technology Research and Development Program 863 (2013AA102207).

References:

[1] Abraham Ulman. *Chem. Rev.*, 1996, **96**, 1533-1554.

[2] Werner Stober, Arthur Fink and Ernst Bohn. *J. Colloid Interf. Sci.*, 1968, **26**, 62-69.

[3] E.F.Vansant, P.Van Der Voot and K.C.Vrancken. *Studies in Surface Science and Catalysis*, 1995, **93**, 199-200.

[4] Jianming Zhang, Shangru Zhai, Bin Zhai, Qingda An and Ge Tian. *J. Sol-Gel Sci. Techn.*, 2012, **64**, 347-357.

[5] Zhanwang Zhu, Xinlin Wei, Feng Xu and Yuanfeng Wang. *Solid State Sci.*, 2012, **14**, 1550-1556.

[6] Yuanyuan Liang, Liming Zhang, Wei Li and Rufu Chen. *Colloid Polym. Sci.*, 2007, **285**, 1193-1199.

[7] Jun Sun, Yujie Su, Shengqi Rao and Yanjun Yang. *J. Chromatogr. B.*, 2011, **879**, 2194-2200.

[8] Fabiana Superti, Maria Grazia Ammendolia, Francesca Berlutti and Piera Valenti. *Bioactive Egg Compounds*, 2007, **7**, 43-50.

[9] Jianping Wu and Alexandra Acero-Lopez. *Food Res. Int.*, 2012, **46**, 480-487.

[10] Hisham R. Ibrahim, Yasushi Sugimoto and Takayoshi Aoki. *BBA-Biomembranes*, 2000, **1523**, 196-205.

[11] P Valenti, G Antonini, M R Fanelli, N Orsi and E Antonini. *Antimicrob Agents CH.*, 1982, **21**, 840-841.

[12] Robert C. Warner and Ione Weber. *J. Bio. Chem.*, 1951, **238**, 173-180.

[13] Thomas Croguennec, Françoise Nau, Stéphane Pezennec, Michel Piot and Gérard Brulé. *Eur. Food Res. Technol.*, 2001, **212**, 296-301.

[14] ChristinaGraf, DirkL.J.Vossen, ArnoutImhof and Alfons van Blaaderen. *Langmuir*, 2003, **19**, 6693-6700.

[15] Teofil Jesionowski, Filip Ciesielczyk and Andrzej Krysztafkiewicz. *Mater. Chem. Phys.*, 2010, **119**, 65-74.

449 [16] Xiaoying Yang, Xiaoyan Zhang, Yanfeng Ma, Yi Huang, Yinsong Wang and
450 Yongsheng Chen. *J. Mater. Chem.*, 2009, **19**, 2710-2714.
451 [17] An-Hui Lu, E.L.Salabas and Ferdi Schüth. *Angew. Chem. Int. Edit.*, 2007, **46**,
452 1222-1244.
453 [18] Xiaohong Sun, Chunming Zheng, Fuxiang Zhang, Yali Yang, Guangjun Wu,
454 Aimin Yu and Naijia Guan. *J. Phys. Chem. C.*, 2009, **113**, 16002-16008.
455 [19] Zhipeng Yu, Yongguang Yin, Wenzhu Zhao, Feng Chen and Jingbo Liu. *J. Sci.*
456 *Food Agr.,* 2014, **62**.912-917.
457 [20] F Toldrá and LML Nollet. *Proteomics in Foods: Principles and Applications*,
458 2012, **17**, 305-323.
459 [21] Dileep A. Omana, Jiapei Wang and Jianping Wu. *J. Chromatogr. B.*, 2010, **878**
460 1771-1776.
461 [22] C. Gue´rin-Dubiard, M. Pasco, A. Hietanen, A. Quiros del Bosque, F. Nau and T.
462 Croguennec. *J. Chromatogr. A.*, 2005, **1090**, 58-67.
463 [23] Graham G and Bates GW. *J. Lab. Clin. Med.*, 1976, **88**, 477-486.
464 [24] Catherine Guérin-Dubiard, Maryvonne Pasco, Daniel Mollé, Colette Désert,
465 Thomas Croguennec and Françoise Nau. *J. Agr. Food Chem.*, 2006, **54**, 3901-3910.

Fig. 1. FTIR spectrums of Fe_3O_4@SiO_2-NH_2 nanoparticles and Fe_3O_4 nanoparticles. The samples were mixed with KBr powder and then made into pellet under high pressure. The sample pellet were scanned from 4000 to 400 cm^{-1}. Pure KBr acted as blank.

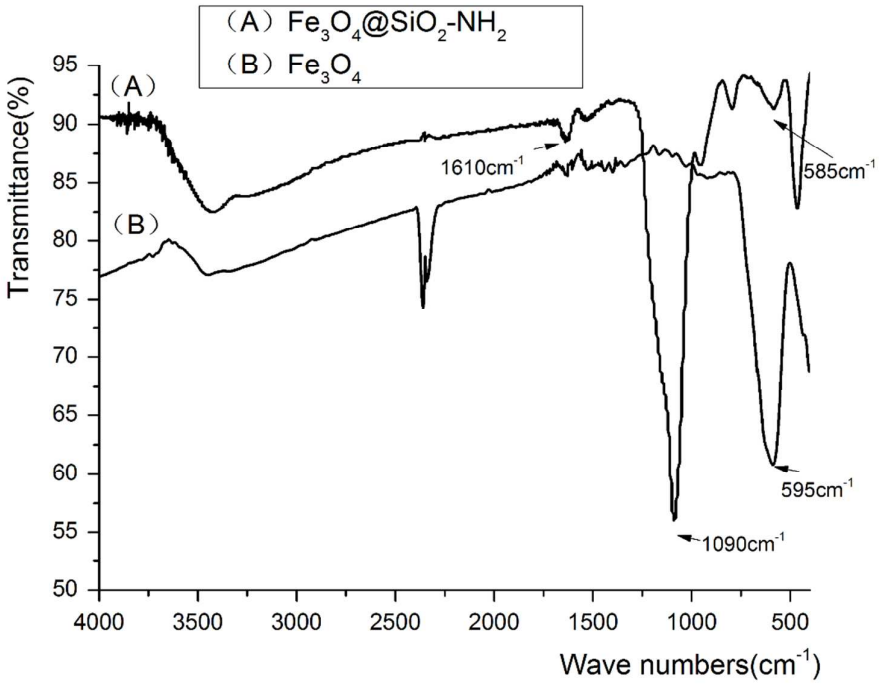

Fig. 2. Size distributions of Fe_3O_4@SiO_2-NH_2 nanoparticles in different medium (pH 4.0, 5.0, 6.0, 7.0, 8.0, 9.0, 10.0).

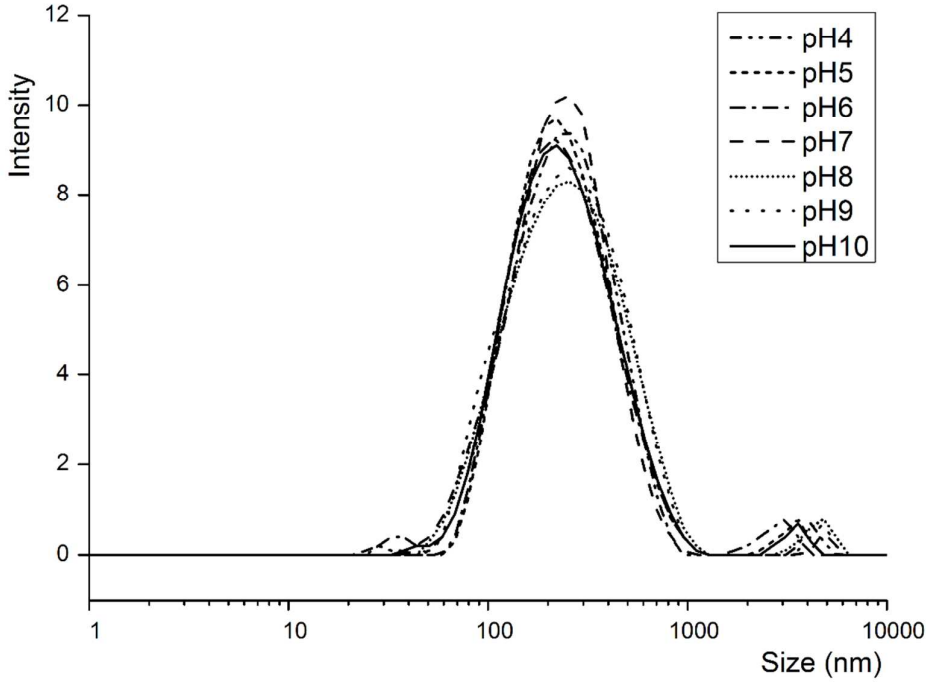

Fig. 3. Zeta potential of Fe_3O_4 nanoparticles and Fe_3O_4@SiO_2-NH_2 particles.

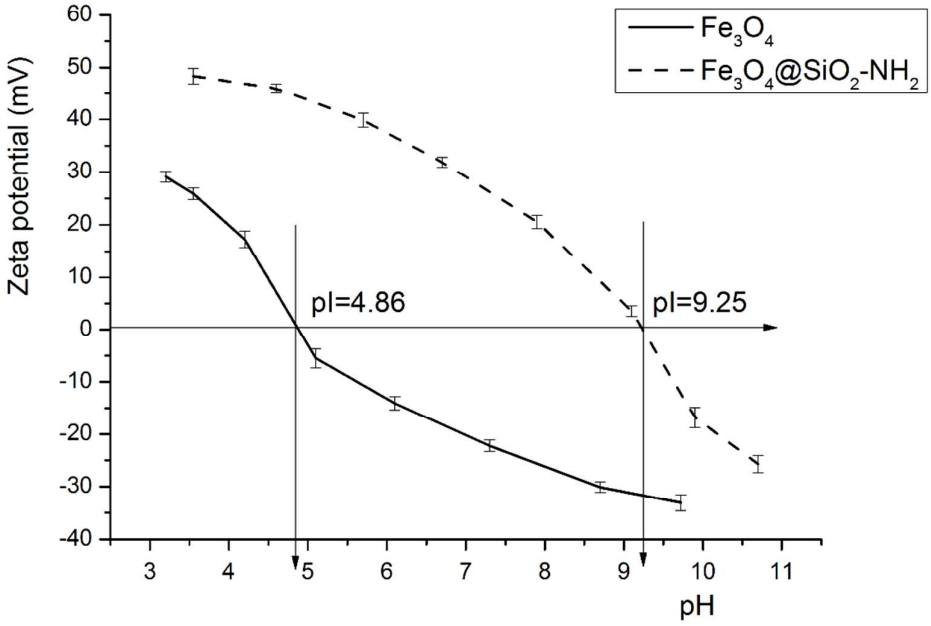

Fig. 4. Effect of APTMS dosage on the zeta potential of Fe_3O_4@SiO_2-NH_2 nanoparticles.

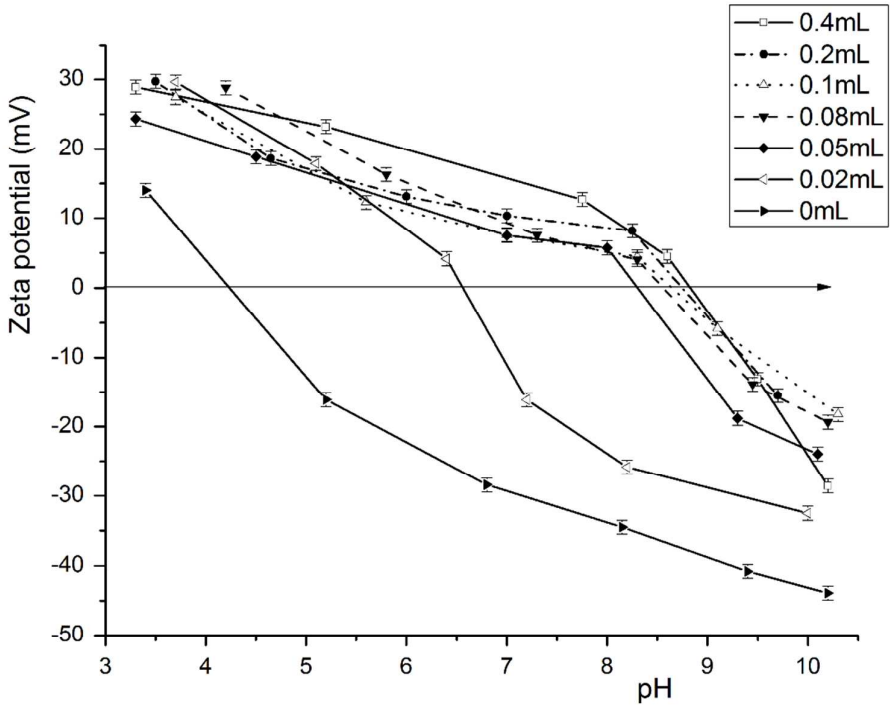

Fig. 5. TEM images of naked Fe_3O_4 nanoparticles (A and B) and Fe_3O_4@SiO_2-NH_2 nanoparticles (C and D).

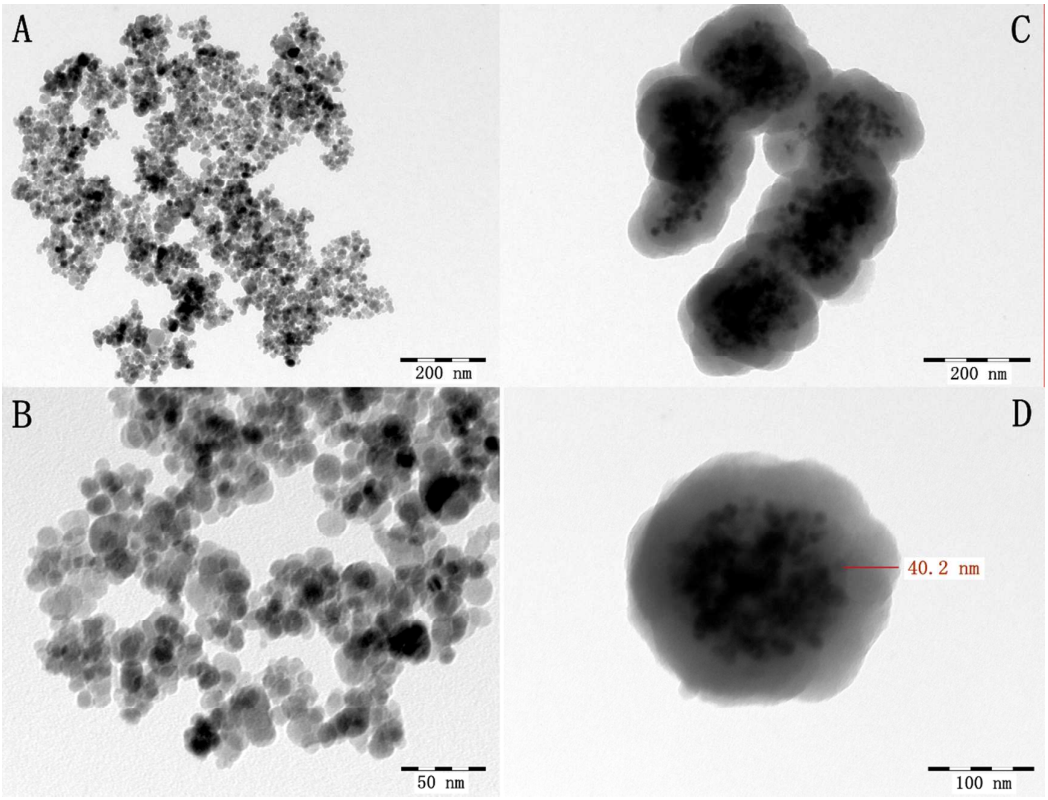

Fig. 6. XRD patterns of naked Fe_3O_4 nanoparticles and Fe_3O_4@SiO_2-NH_2 nanoparticles.

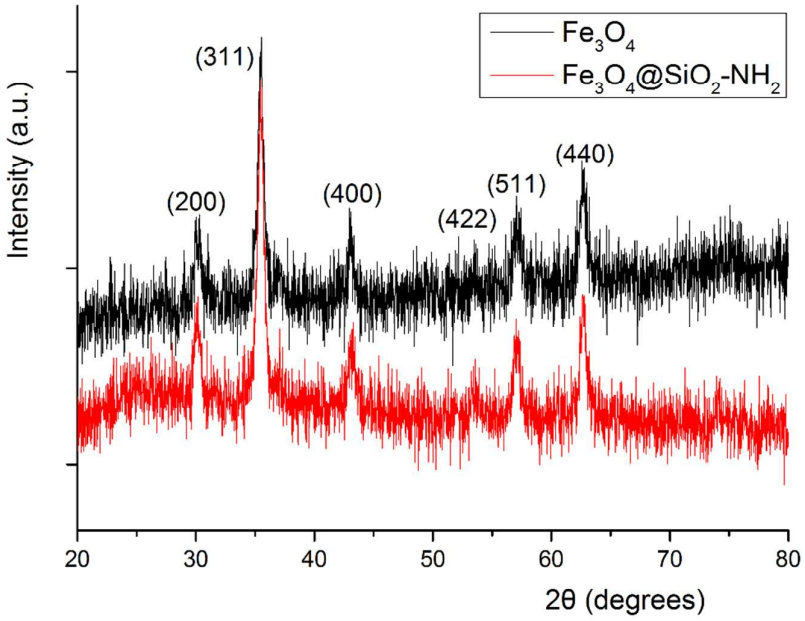

Fig. 7. TGA curves of naked Fe_3O_4 nanoparticles and Fe_3O_4@SiO_2-NH_2 nanoparticles.

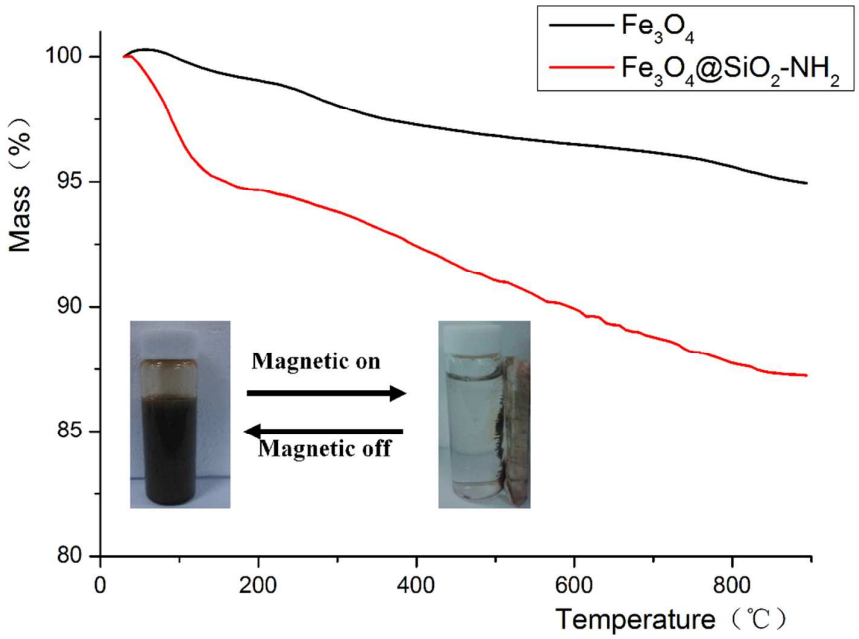

Fig. 8. Effect of temperature on OVT adsorption onto Fe_3O_4@SiO_2-NH_2 nanoparticles; pH 7.4.

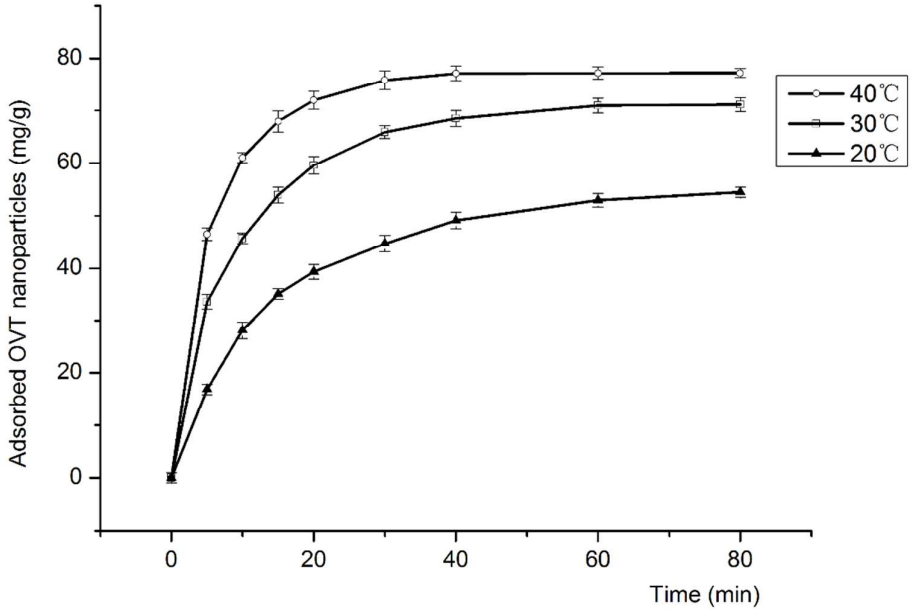

Fig. 9. Effect of pH on the maximum adsorption of OVT onto Fe_3O_4@SiO_2-NH_2 nanoparticles; temperature: 30°C.

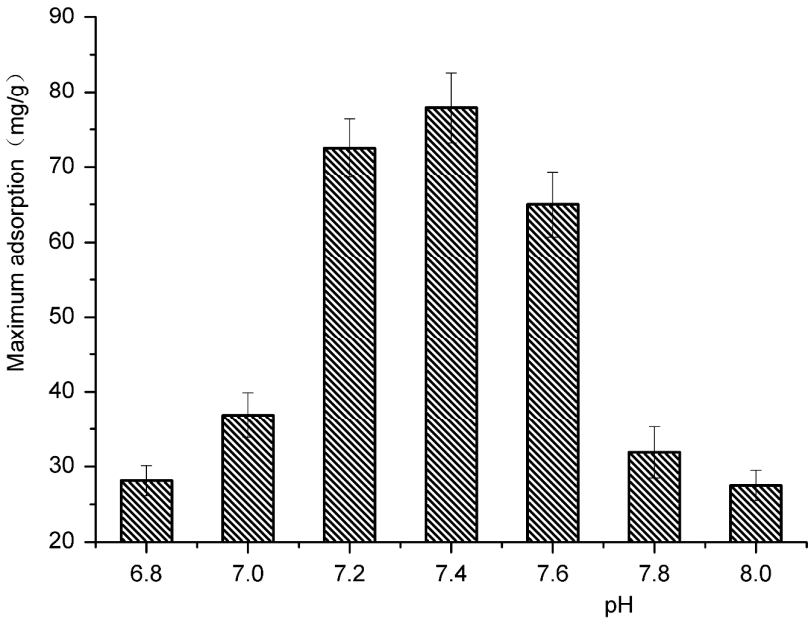

Fig. 10. SDS-PAGE analysis of the eluted protein solution: lane 1, biomarker (sigma), lane 2, natural chicken egg white solution after pretreatment, lanes 3-8, target protein solution adsorbed by Fe_3O_4@SiO_2-NH_2 nanoparticles at different pH (6.8, 7.0, 7.2, 7.4, 7.6, 7.8 from left to right).

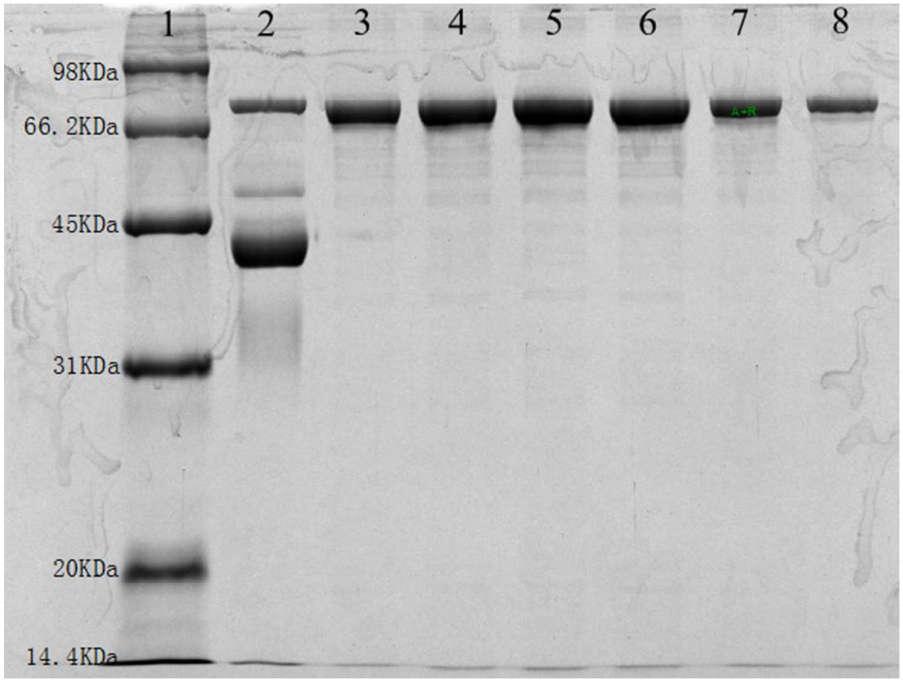

Fig. 11. Saturation curve by iron on OVT.

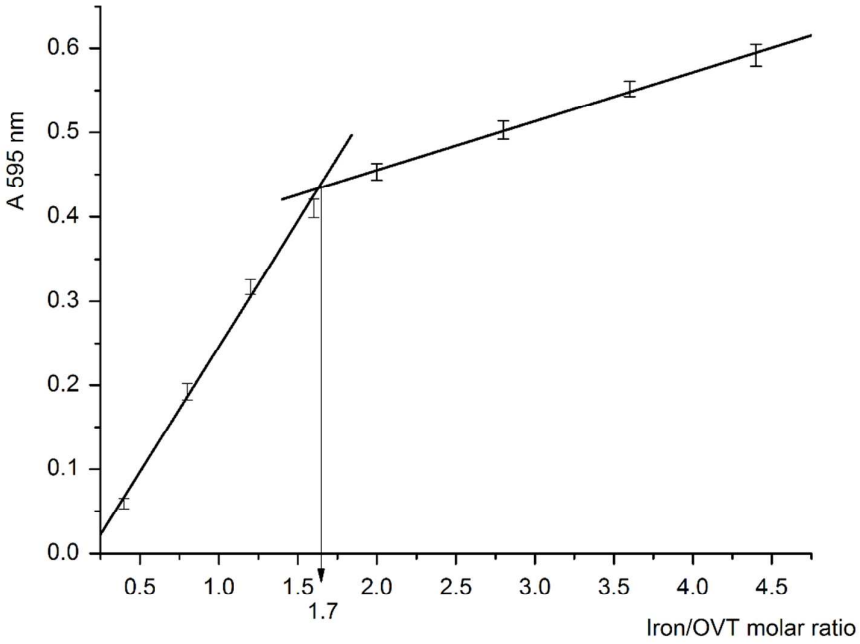

Fig. 12. Maximum adsorption of OVT on Fe_3O_4@SiO_2-NH_2 nanoparticles after repeated for certain times.

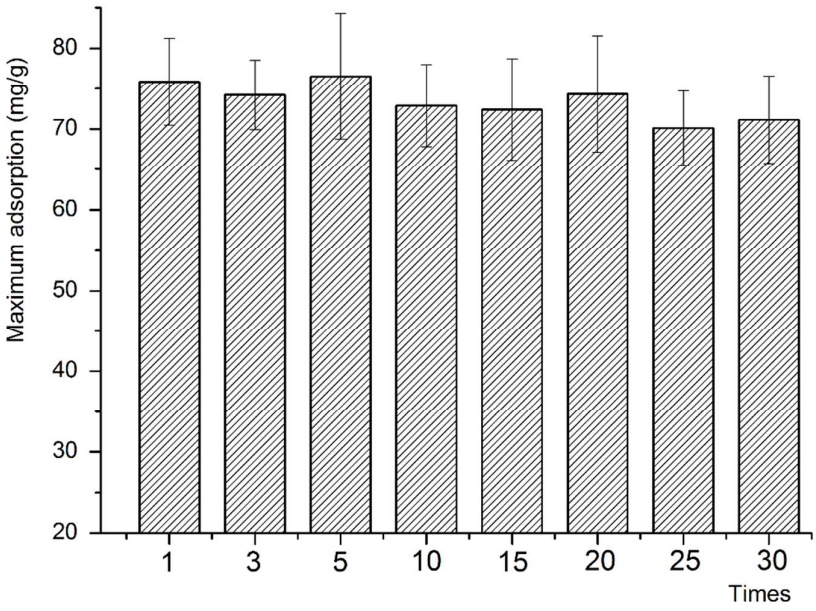

Fig. 13. The recovery of Fe_3O_4@SiO_2-NH_2 nanoparticles in the repeated adsorption-desorption experiments.

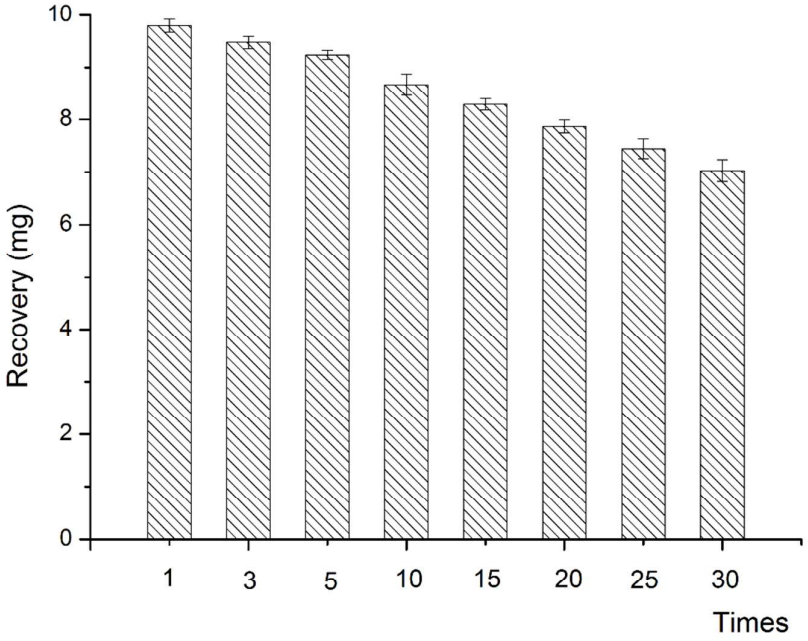

Tab. 1. Mean diameters and pDI of Fe_3O_4@SiO_2-NH_2 nanoparticles in different medium (pH 4.0, 5.0, 6.0, 7.0, 8.0, 9.0, 10.0).

pH	4.0	5.0	6.0	7.0	8.0	9.0	10.0
Mean size (nm)	204.2	201.8	210.6	220.1	205.3	212.4	215.6
pDI	0.322	0.33	0.348	0.333	0.3	0.347	0.354

Scheme 1. Illustration of the synthesis process of Fe_3O_4@SiO_2-NH_2 nanoparticles.

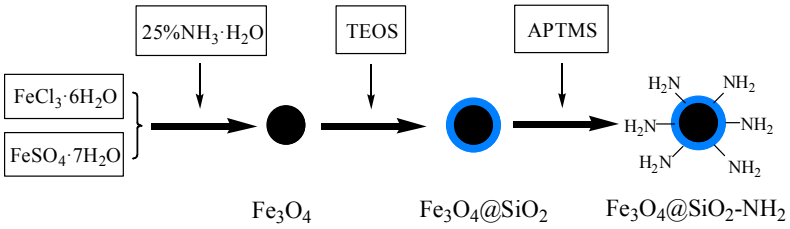

Scheme 2. Demonstration of magnetic manipulation of separation process using the nanoparticles.

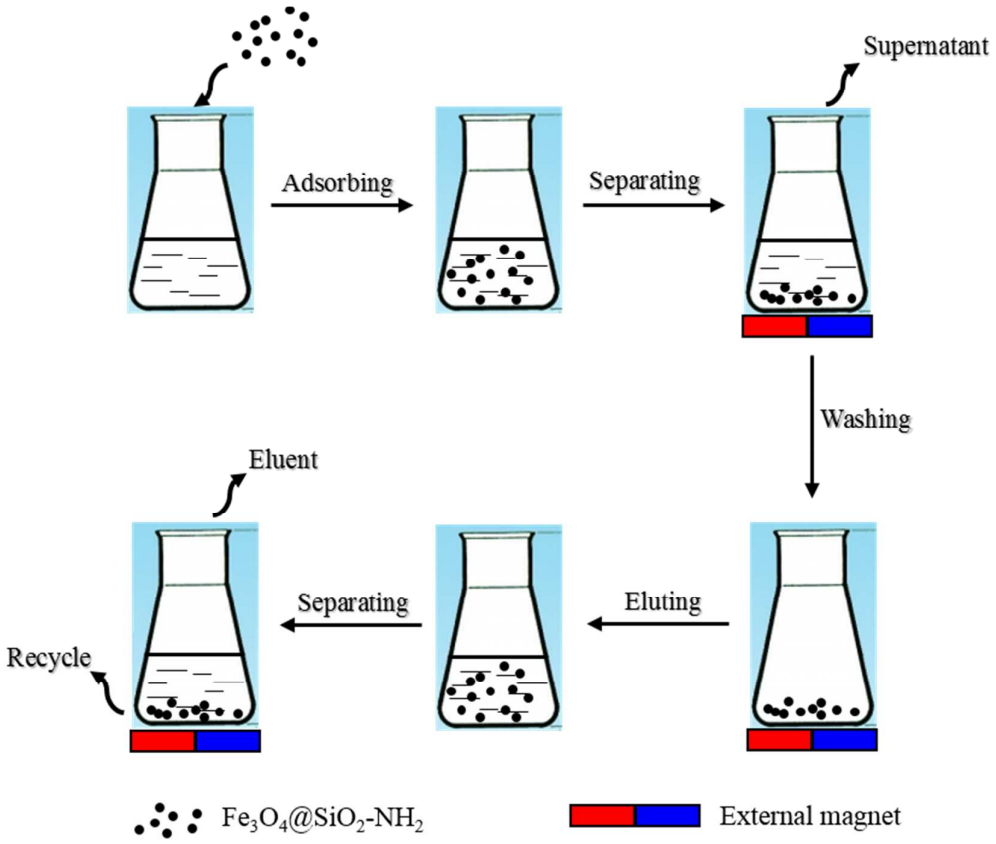

Synthesis, characterization, and application of Fe_3O_4@SiO_2-NH_2 nanoparticles

Feng Liu [a b 1], Fuge Niu [a b], Ning Peng [a b], Yujie Su [a b *], Yanjun Yang [a b *]

[a] State Key Laboratory of Food Science and Technology, Jiangnan University, Wuxi 214122, PR China

[b] School of Food Science and Technology, Jiangnan University, Wuxi 214122, PR China

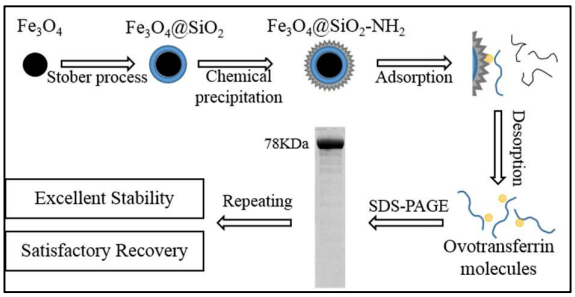

Synthesis of Fe_3O_4@SiO_2-NH_2 nanoparticles by a mild and time-saving method and the application in separation of ovotransferrin were studied.